Available online at www.sciencedirect.com
SCIENCE DIRECT®
Journal of Catalysis 233 (2005) 1–15
JOURNAL OF CATALYSIS
www.elsevier.com/locate/jcat

CO_2 activation and synthesis of cyclic carbonates and alkyl/aryl carbamates over adenine-modified Ti-SBA-15 solid catalysts

R. Srivastava, D. Srinivas *, P. Ratnasamy *

National Chemical Laboratory, Pune-411 008, India

Received 3 December 2004; revised 15 March 2005; accepted 18 March 2005

Available online 23 May 2005

Abstract

Cyclic carbonates were synthesized by the cycloaddition of CO_2 to epoxides (epichlorohydrin, propene oxide, and styrene oxide), and carbamates were synthesized by reaction of alkyl or aryl amines, CO_2, and *n*-butyl bromide. Solvents and cocatalysts/promoters like N,N-dimethylaminopyridine (DMAP) and quaternary ammonium salts, which are usually essential with conventional catalyst systems, could be avoided with the use of adenine-modified Ti-SBA-15 catalysts. The catalysts were reused in several recycle experiments. The structural and textural properties of the catalysts were determined by X-ray diffraction (XRD), transmission electron microscopy (TEM), N_2 adsorption, and Fourier transform infrared (FTIR) and diffuse reflectance ultraviolet–visible (UV–vis DRS) techniques. Acid–base properties of the solid catalysts were investigated by temperature-programmed desorption (TPD) of NH_3 and CO_2 and DRIFTIR spectroscopy of adsorbed pyridine and CO_2 techniques. The studies reveal that the Ti^{4+} ions increase catalytic activity by enhancing the adsorption of the epoxide and alkyl or aryl amine substrates. CO_2 molecules are activated at the basic nitrogen groups of adenine. Increasing the surface concentrations of either CO_2 (by anchoring basic molecules like adenine or increasing the partial pressure of CO_2) or epoxides and alkyl or aryl amines (by increasing the concentration of Lewis acidic Ti^{4+} ions) enhances the catalytic activity. CO_2 molecules activated at the covalently anchored adenine sites react with epoxide/amines adsorbed on the silica surface to form carbonates/carbamates.

Keywords: CO_2 fixation; Activation of CO_2; Synthesis of cyclic carbonates; Synthesis of carbamates; Phosgene-free synthesis; DRIFTIR spectroscopy of adsorbed pyridine and CO_2; Temperature-programmed desorption of NH_3 and CO_2; Titanosilicates; Organo-functionalized mesoporous silica; Ti-SBA-15

1. Introduction

Efficient transformation of CO_2 into useful chemicals is an area of contemporary interest [1,2]. The insertion of CO_2 in the oxirane ring of epoxides is a powerful method for CO_2 fixation and utilization to produce five-membered, cyclic carbonates

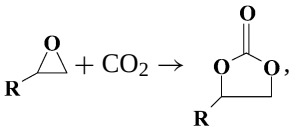

(1)

R = –CH_2Cl, –CH_3 or –C_6H_5.

The latter are used as polar aprotic solvents, electrolytes in secondary batteries, precursors for polycarbonate materials, and, in general, intermediates in organic synthesis [3–7].

Several homogeneous complexes catalyze the CO_2-epoxide cycloaddition reaction [8–13]. Several heterogeneous catalysts, such as polystyrene-bound onium salts [14], basic metal oxides [15,16], Mg–Al mixed oxides [17], Nb(IV) and Nb(V) catalysts [18], lanthanide oxychlorides [19], alkali metal-loaded zeolites and alumina [20,21], poly(4-vinylpyridine)-supported zinc halide [22], ionic liquids [23–25], silica-supported guanidine [26], and Schiff base and phthalocyanine complexes covalently bonded to porous silica [27,28], have also been reported. Commercial production of cyclic carbonates by a nonphosgene route with quaternary ammonium salt-based catalysts has been announced recently by BASF [29] and Chimei-Asahi Corporation (Tai-

* Corresponding authors. Fax: +91 020 2589 3761.
E-mail addresses: d.srinivas@ncl.res.in (D. Srinivas), p.ratnasamy@ncl.res.in (P. Ratnasamy).

0021-9517/$ – see front matter
doi:10.1016/j.jcat.2005.03.023

wan) [30]. However, with most of the above-mentioned solid catalysts and with the commercial quaternary ammonium salt catalyst, the reaction had to be carried out at high temperatures/pressures (30–80 bar) for high yields. In some cases a solvent was also essential for high carbonate selectivity. Earlier, we reported the application of zeolite-based catalysts (encapsulated metal phthalocyanines and titanosilicates TS-1 and Ti-MCM-41) for this reaction [31–33]. Although solventless operation at medium temperatures and pressures (393 K, 6.9 bar) was feasible with the zeolite-based catalysts [31–33], they still required an additional homogeneous cocatalyst/promoter, N,N-dimethylaminopyridine (DMAP), for high activity. In the present study, we report a novel, reusable, solid catalyst system, nucleobase (adenine)-modified, mesoporous Ti-SBA-15 (Ti-SBA-15-*pr*-Ade), which, while retaining the advantages of the solid catalysts reported by us earlier [31–33], also avoids the use of any additional cocatalyst/promoter. It is also equally efficient and reusable under mild reaction conditions.

Carbamates represent another important class of organic compounds that are used in a variety of applications, including polyurethanes, pesticides, fungicides, medicinal drugs, and synthetic intermediates [34]. They are commercially manufactured with the use of toxic phosgene and isocyanate intermediates [35,36]. Alternative, nonphosgene routes to carbamates like reductive carbonylation (with expensive platinum group metal catalysts) [37], oxidative carbonylation [38,39], and methoxycarbonylation of amine [40] (involves separation of methanol-DMC azeotrope, an expensive operation) all have significant disadvantages. The reaction of primary amines, CO_2, and alkyl halides is a benign route to carbamates synthesis

$$2RNH_2 + CO_2 \rightleftharpoons [RNHCOO^-][RNH_3^+], \quad (2)$$

$$[RNHCOO^-][RNH_3^+] + n\text{-BuBr} \rightarrow RNH\text{–}\overset{\overset{O}{\|}}{C}\text{–}O(n\text{-Bu}) + RNH_2 + HBr,$$

R = alkyl or aryl; *n*-Bu = *n*-butyl.

Various homogeneous catalysts like organic and inorganic bases, crown ethers, and cryptands catalyze this reaction [41–44]. Earlier, we had found [45] that zeolite-encapsulated metal complexes and titanosilicates also catalyze this reaction very efficiently. However, the reaction had to be conducted in a solvent such as N,N-dimethyl formamide (DMF) for high carbamate yields. We now report the synthesis of carbamates under solvent-free conditions over adenine-modified Ti-SBA-15 solid catalysts. To the best of our knowledge, this is the first case where an organofunctionalized mesoporous titanosilicate has been used to catalyze the formation of carbonates and carbamates, with the use of CO_2 as the raw material. The causes of the superior catalytic activity of Ti-SBA-15-*pr*-Ade are probed by FTIR spectroscopy and temperature-programmed desorption techniques. The various catalytic reactions investigated are listed below.

Cyclic carbonates:

- Epichlorohydrin + CO_2 → Chloropropene carbonate
- Propene oxide + CO_2 → Propene carbonate
- Styrene oxide + CO_2 → Styrene carbonate

Alkyl and aryl carbamates:

- Aniline + CO_2 + *n*-butyl bromide → *n*-butyl-N-phenyl carbamate
- 2,4,6-Trimethylaniline + CO_2 + *n*-butyl bromide → *n*-butyl-N-2,4,6-trimethylphenyl carbamate
- Benzylamine + CO_2 + *n*-butyl bromide → *n*-butyl-N-methylphenyl carbamate
- Cyclohexylamine + CO_2 + *n*-butyl bromide → *n*-butyl-N-cyclohexyl carbamate
- Hexylamine + CO_2 + *n*-butyl bromide → *n*-butyl-N-hexyl carbamate
- Octylamine + CO_2 + *n*-butyl bromide → *n*-butyl-N-octyl carbamate

2. Experimental

2.1. Catalyst preparation

2.1.1. SBA-15

Mesoporous silica SBA-15 was synthesized according to the reported procedure [46,47]. In a typical synthesis, 2 g of amphiphilic triblock copolymer, poly (ethylene glycol)-block-poly(propylene glycol)-block-poly(ethylene glycol) ($EO_{20}PO_{70}EO_{20}$; average molecular weight = 5800; Aldrich Co.), was dispersed in 15 g of water and 60 g of 2 M HCl solution with stirring, followed by the addition of 4.25 g of tetraethyl orthosilicate (TEOS) (Aldrich Co.) to the homogeneous solution**.** This gel was continuously stirred at 313 K for 24 h and finally crystallized in a Teflon-lined steel autoclave at 373 K for 2 days. After crystallization, the solid product was centrifuged, filtered, washed with deionized water, and dried in air at room temperature (298 K). The material was calcined at 823 K for 6 h to decompose the triblock copolymer and obtain a white powder, SBA-15.

2.1.2. Ti-SBA-15

Ti-incorporated SBA-15 (Ti-SBA-15) was prepared by a postsynthesis method [47] with the use of tetrabutyl orthotitanate (95 wt% TBOT; Aldrich Co.) as a Ti source. In a typical preparation, a certain amount of TBOT was hydrolyzed in 40 cm^3 of glycerol (99 wt%, s. d. fine Chem. Ltd.) containing 7.5 cm^3 of tetrapropylammonium hydroxide (TPAOH) (20 wt%; Aldrich Co.), to obtain a homogeneous solution. To this solution was added 2 g of SBA-15 without any pretreatment, and the mixture was heated statically at 373 K for 72 h to induce titanation. Ti-SBA-15, thus obtained, was filtered and washed with deionized water, and the organic species were burned off at 773 K for 4 h. Four

batches of Ti-SBA-15 (A–D) with final Si/Ti compositions of 119, 104, 68, and 40 were prepared.

2.1.3. SBA-15-pr-Cl, SBA-15-pr-NH_2, Ti-SBA-15-pr-Cl, and Ti-SBA-15-pr-NH_2

In a typical organo-functionalization [48,49], SBA-15 was activated under vacuum at 423 K for about 3 h. 3-Chloro or 3-amino-propyltriethoxysilane (9 mmol/3 g of SBA-15; Lancaster) in 100 cm^3 of dry toluene was added to it and refluxed under nitrogen for 6 h. Soxhlet extraction with dichloromethane (for 12 h) and then with acetone (for 12 h) yielded Cl- and NH_2-functionalized SBA-15 materials, SBA-15-*pr*-Cl and SBA-15-*pr*-NH_2, respectively.

Ti-SBA-15-*pr*-Cl and Ti-SBA-15-*pr*-NH_2 were prepared in a similar manner, with the use of Ti-SBA-15 in place of SBA-15. Nitrogen content (elemental analysis) – Final/output (input, mmol/g): SBA-15-*pr*-NH_2, 2.45 (3.0); Ti-SBA-15-*pr*-NH_2 (Si/Ti = 40), 2.2 (3.0).

2.1.4. SBA-15-pr-Ade and Ti-SBA-15-pr-Ade

Adenine (1.76 mmol, 0.238 g) was taken in 30 cm^3 of dry DMF and stirred for 30 min under nitrogen at 393 K for complete dissolution. Then, 1.5 g of SBA-15-*pr*-Cl or Ti-SBA-15-*pr*-Cl was added and stirring was continued for 12 h. The solid was filtered and Soxhlet extracted with DMF (for 10 h) and then with CH_3CN (for 12 h). Nitrogen content (elemental analysis) – Final/output (input, mmol/g): SBA-15-*pr*-Ade, 1.29 (1.76); Ti-SBA-15-*pr*-Ade (Si/Ti = 104), 0.96 (1.76); Ti-SBA-15-*pr*-Ade (Si/Ti = 68), 0.95 (1.76); Ti-SBA-15-*pr*-Ade (Si/Ti = 40), 0.91 (1.76). The synthetic procedure is summarized in Scheme 1.

2.2. Catalyst characterization

Titanium content was estimated with a Rigaku 3070 E wavelength dispersive X-ray fluorescence (XRF) spectrometer with a Rh target energized at 50 kV and 40 mA. The organic content (C, H, and N) in the modified SBA-15 samples was estimated by a Carlo-Erba 1106 elemental analyzer. XRD patterns were recorded on an X'Pert Pro (Philips) diffractometer with Cu-K_α radiation and a proportional counter as a detector. A divergent slit of 1/32° on the primary optics and an antiscatter slit of 1/16° on the secondary optics were used to measure the data in the low-angle region. Transmission electron microscopy (TEM) of the samples was done on a JEOL (model 1200 EX) microscope operating at 100 kV. A calcined sample was dispersed in isopropyl alcohol, deposited on a Cu grid, and dried. The specific surface area (S_{BET}) of the samples was determined by N_2 adsorption at 77 K (NOVA 1200 Quanta Chrome equipment). Before N_2 adsorption, the samples were evacuated at 573 K. S_{BET} was determined from the linear part of the BET equation ($p/p_0 = 0.05$–0.31). The pore size distribution was calculated with the Barrett–Joyner–Halenda (BJH) method.

UV–vis DRS spectra of the samples were obtained with a Shimadzu spectrophotometer (UV-2500 PC). In CO_2 adsorption studies using FTIR spectroscopy (Shimadzu 8201 PC spectrophotometer in the region 400–4000 cm^{-1}), the samples were made into a paste with dichloromethane and then exposed to CO_2 under different experimental conditions (temperature = 253–298 K; CO_2 pressure = 2–20 bar; time = 1 h). The spectra before and after CO_2 adsorption were recorded in diffuse reflectance mode (spectral resolution = 4 cm^{-1}; number of scans = 100). We obtained the difference spectrum by subtracting the spectrum of the unexposed SBA sample from that of the corresponding CO_2 adsorbed sample.

FTIR spectra for adsorbed pyridine were recorded with a Shimadzu SSU 8000 DRIFTIR spectrophotometer equipped with a liquid-nitrogen-cooled MCT detector. Samples were activated at 573 K for SBA-15 and Ti-SBA-15 and at 473 K for those containing the amines. They were then cooled to 323 K, and pyridine (0.03 cm^3) was adsorbed. The sample temperature was raised and held at the desired value for 30 min before the spectrum was recorded (spectral resolution = 4 cm^{-1}; number of scans = 100). We obtained difference spectra by subtracting the spectrum of the catalyst from that of corresponding pyridine-adsorbed samples.

Temperature-programmed desorption (TPD) experiments were conducted on a Micromeritics AutoChem 2910 instrument. In a typical experiment, 120 mg of sample was placed in a U-shaped, flow-through, quartz sample tube. Before the TPD experiments, the catalyst was pretreated in He (50 cm^3/min) at 473 K for 1 h. A mixture of NH_3 in He (10:90) was then passed (75 cm^3/min) at 353 K for 1 h. The sample was subsequently flushed in He (50 cm^3/min) at 383 K for 2 h to remove physisorbed ammonia. The TPD experiments were carried out in the range of 323–623 K at a heating rate of 10 K/min. The ammonia concentration in the effluent was monitored with a gold-plated, filament thermal conductivity detector. The areas under the peaks were integrated with the software GRAMS/32 to determine the amount of desorbed ammonia.

In CO_2-TPD experiments the catalyst was pretreated at 473 K for 1 h. CO_2 was adsorbed at 300 K for 1 h. The sample was then flushed for 1 h to remove physisorbed CO_2. The TPD was carried from 298 to 523 K at a heating rate of 10 K/min. The sample was kept at 523 K for 30 min.

In various amine and epoxide adsorption measurements, the solid catalysts (100 mg) were brought into contact with 3 cm^3 of 10 wt% CH_3CN solutions of amines or 10 wt% of CH_2Cl_2 solutions of epichlorohydrin (epoxide) at 298 K for 1 h. The amount of the amine or epoxide adsorbed to the solid catalyst was estimated by analysis of the liquid portion (after the adsorption experiments) by gas chromatography (Varian 3400; CP-SIL8CB column).

2.3. Reaction procedure

2.3.1. Cyclic carbonates

In a typical cycloaddition reaction, epoxide (18 mmol), catalyst (100 mg), and solvent (0 or 10 cm^3) were placed

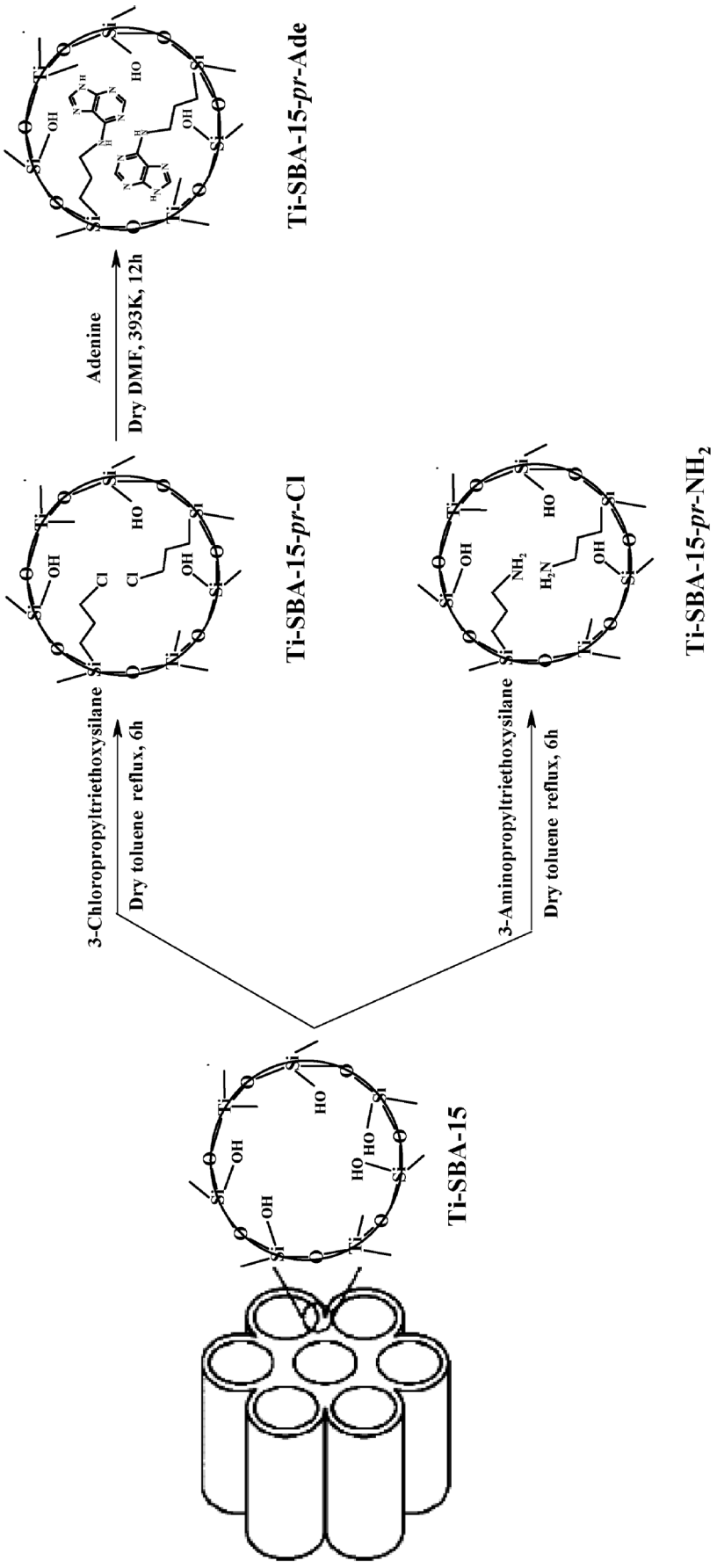
Ti-SBA-15
3-Chloropropyltriethoxysilane
Dry toluene reflux, 6h
Ti-SBA-15-pr-Cl
Adenine
Dry DMF, 393K, 12h
Ti-SBA-15-pr-Ade
3-Aminopropyltriethoxysilane
Dry toluene reflux, 6h
Ti-SBA-15-pr-NH2

Scheme 1.

in a 300 cm^3 stainless-steel PARR reactor. The reactor was pressurized with CO_2 (6.9 bar), the temperature was raised to 393 K, and the reaction was conducted for 4–8 h. The reactor was then cooled to room temperature, unreacted CO_2 was vented out, catalyst was separated by centrifugation, and the products were isolated and analyzed by gas chromatography (Varian 3400; CP-SIL8CB column; 30-m long, 0.53-mm i.d.). The products were identified by GC-MS (Shimadzu QP-5000; with a 30-m long, 0.25-mm i.d., 0.25-μm thick capillary column DB-1), GC-IR (Perkin Elmer 2000; BP-1 column; with a 25-m long, 0.32-mm i.d.), and ^{1}H NMR (Bruker AC 200). The reaction was carried out with several epoxides (epichlorohydrin, propene oxide, and styrene oxide).

2.3.2. Alkyl and aryl carbamates

n-Butyl-N-phenyl carbamate. In a typical reaction, aniline (10 mmol), *n*-butyl bromide (12 mmol), and catalyst (100 mg) were charged into a 300 cm^3 PARR reactor. The reactor was then pressurized with CO_2 (3.4 bar), and the temperature was raised to 353 K. The reaction was conducted for 4 h. At the end, the reactor was cooled to 298 K and unused CO_2 was vented out. The catalyst was recovered from the reaction mixture by filtration. The products were analyzed by thin-layer chromatography (TLC) and gas chromatography and identified by GC-MS, FTIR, and ^{1}H NMR as described above. Other carbamates were synthesized and characterized in a similar manner.

3. Results and discussion

3.1. Structural and textural properties

Ti-SBA-15 (Si/Ti = 40–119) was prepared by the post-synthesis method [47]. It was then organo-functionalized with 3-chloropropyltriethoxysilane to get Ti-SBA-15-*pr*-Cl [48,49]. Further reaction with adenine (under water-free, inert conditions) yielded Ti-SBA-15-*pr*-Ade (Scheme 1). For comparative studies, we prepared Ti-SBA-15-*pr*-NH_2 samples by reacting Ti-SBA-15 with 3-aminopropyltriethoxysilane.

The small-angle XRD profiles of SBA-15 materials (Fig. 1) showed three well-resolved peaks, in agreement with the earlier reports [47], in the 2θ range of 0.8–2°, which could be indexed according to a 2D hexagonal *p6mm* symmetry. The low-angle peak corresponding to the (100) reflection broadened and reduced in intensity on encapsulation of adenine because of pore filling. The catalysts showed type IV nitrogen adsorption–desorption isotherms with H1 hysteresis (Fig. 2). The sharp increase in adsorption at $p/p_0 \approx 0.68$ confirms a highly ordered mesoporous structure. The pore size distribution is very narrow. The physical properties of the materials are listed in Table 1. On introduction of Ti and adenine, the following changes were noted: (a) the surface area (S_{BET}) decreased from 871 to 627 m^2/g, (b) the

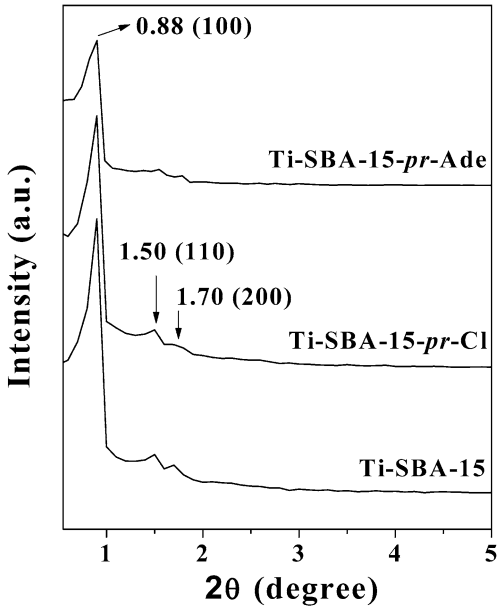

Fig. 1. XRD profiles of Ti-SBA-15, Ti-SBA-15-*pr*-Cl, and Ti-SBA-15-*pr*-Ade; Si/Ti = 40.

total pore volume decreased from 1.55 to 1.04 cm^3/g, and (c) the average pore diameter decreased from 7.2 to 6.5 nm. Transmission electron microscopy (TEM) (Fig. 3) further established the 2D hexagonal pore arrays and mesostructure of the modified SBA-15 materials. The pore diameter estimated from TEM measurements (∼ 8 nm) agrees well with that obtained (7.2 nm) with the nitrogen adsorption (BJH) method (Fig. 2). The characterization studies thus reveal that the long-range ordering and mesostructural arrangement of SBA-15 are not significantly disturbed because of organo-functionalization.

3.2. Surface acidity and basicity

The acidity of the catalysts was studied with pyridine and NH_3 as probe molecules. There is an increase in the amount of NH_3 desorbed on going from SBA-15 (0.34 mmol/g) to Ti-containing samples (0.9, 0.9, 1.0 mmol/g, for Ti-SBA-15, Ti-SBA-*pr*-NH_2, and Ti-SBA-*pr*-Ade, respectively). To characterize the nature of the acid centers in more detail, the FTIR spectra of pyridine adsorbed on these samples were recorded (Fig. 4). Fig. 4a indicates the absence of Brønsted (1546 and 1639 cm^{-1}) and strong Lewis (1623 and 1455 cm^{-1}) acid sites. Only weak Lewis (1486 and 1577 cm^{-1}) acid sites (probably associated with the Ti^{4+} ions) were present. In addition, peaks around 1595 and 1445 cm^{-1} due to hydrogen-bonded pyridine were also observed. SBA-15 does not possess any Brønsted or Lewis acid sites, whereas the Ti samples contained only weak Lewis acid sites. Fig. 4b illustrates the expected decrease in the intensity of adsorbed pyridine at higher temperatures. Fig. 4c compares the intensity of the pyridine peaks of the fresh sample with that obtained after the tenth recycle (see Section 3.5.1). There is no major difference between the two

Table 1
Composition and physical characteristics of Ti-SBA-15 samples

Sample	SiO_2/TiO_2 (mole ratio)		XRD d_{100} (nm)	Unit cell parameter (nm)	S_{BET} (m^2/g)	Pore diameter (nm)	Total pore volume (cm^3/g)	Mesopore volume (cm^3/g)	Micropore volume (cm^3/g)	Wall thickness (nm)
	Gel	Product (XRF)								
SBA-15	∞	–	9.8	11.3	871	7.2	1.55	1.44	0.11	4.1
Ti-SBA-15 (A)	50	119	10.1	11.6	794	6.5	1.29	1.19	0.10	5.1
Ti-SBA-15 (B)	30	68	10.1	11.6	770	6.7	1.29	1.19	0.10	4.9
Ti-SBA-15 (C)	20	40	10.3	11.8	662	6.5	1.07	0.99	0.08	5.3
Ti-SBA-15-*pr*-Cl	20	40	10.1	11.6	672	7.1	1.18	1.18	0.04	4.5
Ti-SBA-15-*pr*-Ade	20	40	10.0	11.6	627	6.7	1.04	0.96	0.08	4.3

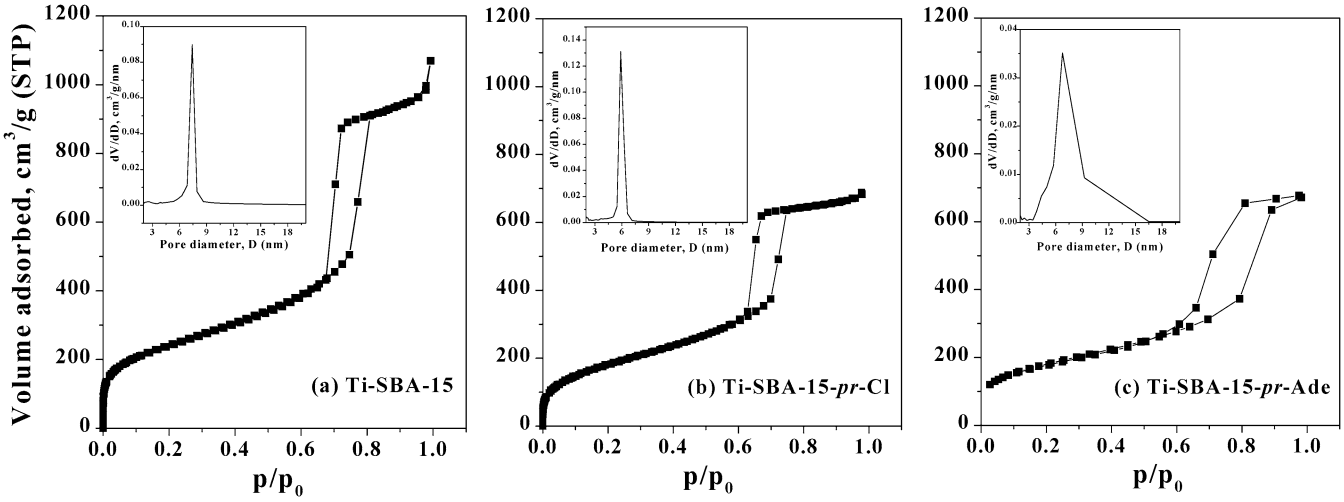

Fig. 2. Nitrogen adsorption–desorption isotherms. Inset shows the pore size distribution.

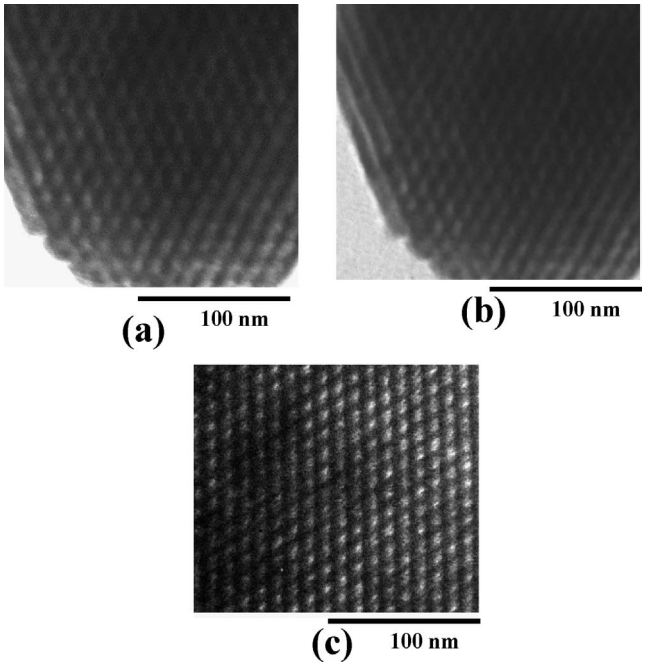

Fig. 3. TEM images of (a) SBA-15, (b) Ti-SBA-15 (Si/Ti = 40), and (c) Ti-SBA-15-*pr*-Ade (Si/Ti = 40).

curves, suggesting the absence of Ti (the probable weakly acidic sites for the adsorption of pyridine) leaching during reaction and regeneration in these samples.

Surface basicity was studied by adsorption of CO_2, an "acidic" molecule. The CO_2 uptake was similar (around 2.9 mmol/g of catalyst) for both SBA-15 and Ti-SBA-15; incorporation of Ti does not affect the basicity of the solid. Surface (OH) groups are probably the sites of CO_2 adsorption. When the amine functions are grafted on the surface, the amount of CO_2 adsorbed increased to 3.8 (for SBA-15-*pr*-NH_2 and Ti-SBA-15-*pr*-NH_2), 4.3 (for SBA-15-*pr*-Ade), or 5.3 mmol of CO_2/g of catalyst (for Ti-SBA-15-*pr*-Ade), respectively. In terms of millimoles of CO_2 adsorbed *per mole of grafted amine molecule*, the values for the above four catalysts were 0.9, 1.0, 1.4, and 2.4, respectively. The similar values for SBA-15-*pr*-NH_2 and Ti-SBA-15-*pr*-NH_2 and the higher values for adenine-grafted samples (compared with *pr*-NH_2 grafted samples) are not surprising. The increase (from 1.4 to 2.4 mmol/mmol) on the Ti-containing sample is interesting, however; it suggests a synergistic interaction between surface acidic (Ti ions) and basic (grafted amine molecules) sites on the adsorption of CO_2.

3.3. Spectral properties

The nature and location of adenine in modified SBA-15 samples were probed by spectral studies. FTIR and UV–vis DRS provided evidence for a strong interaction of the N–H bond in adenine with the modified Ti-SBA-15 surface. In the N–H stretching region, "neat" adenine showed two IR

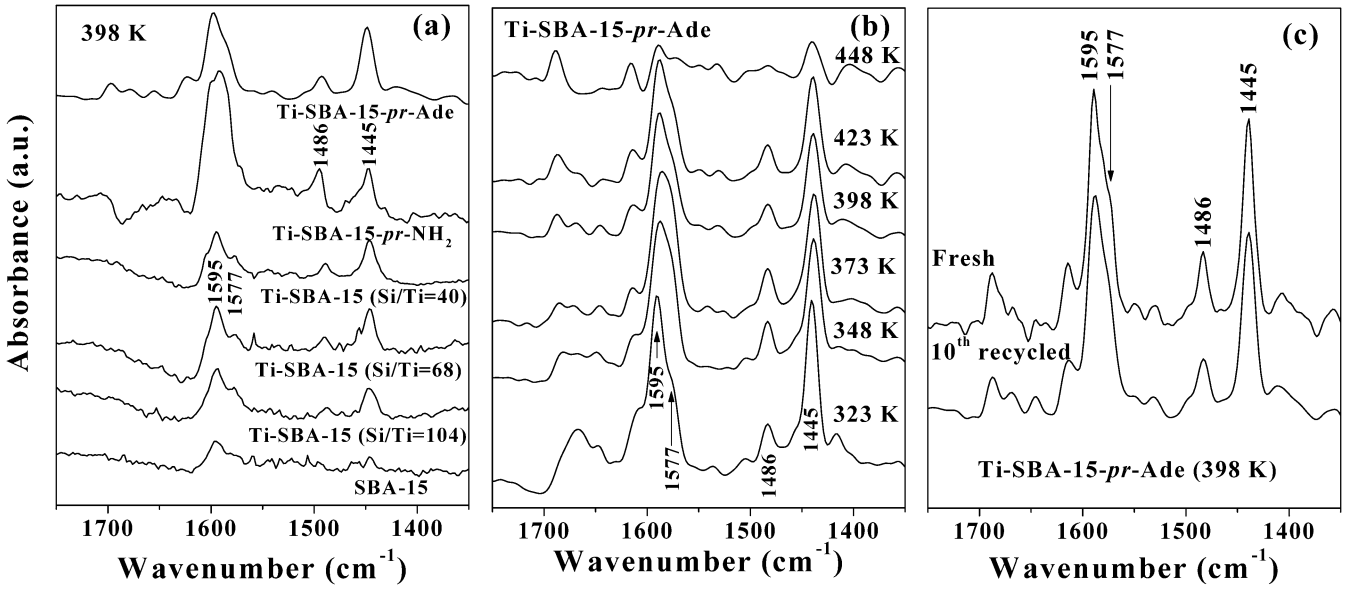

Fig. 4. DRIFTIR spectra of adsorbed pyridine (a) on different catalysts at 398 K, (b) on Ti-SBA-15-*pr*-Ade (Si/Ti = 40) at various temperatures, and (c) on fresh and tenth recycled Ti-SBA-15-*pr*-Ade (Si/Ti = 40) catalysts at 398 K. Spectral resolution, 4 cm^{-1}. Number of scans, 100.

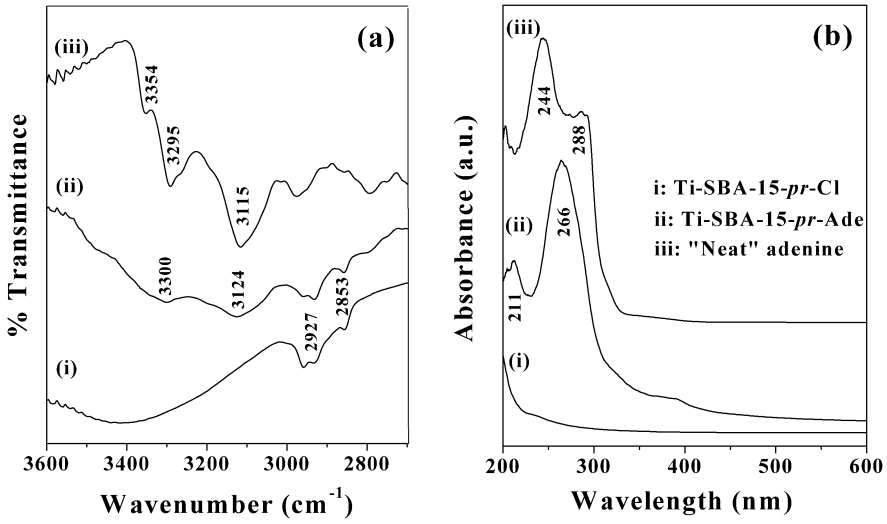

Fig. 5. (a) FTIR and (b) UV–vis. DRS spectra of (i) Ti-SBA-*pr*-Cl, (ii) Ti-SBA-15-*pr*-Ade, and (iii) "neat" adenine.

bands at 3354 and 3295 cm^{-1} corresponding to asymmetric and symmetric N–H stretching vibrations, respectively (Fig. 5a). The covalently linked adenine in Ti-SBA-15-*pr*-Ade, in contrast, showed only one band, at 3300 cm^{-1} (Fig. 5a). Again, pure adenine showed two characteristic UV bands at 244 and 288 nm due to π–π^* and n–π^* transitions (Fig. 5b). Ti-SBA-15-*pr*-Ade showed only a single asymmetric feature with a maximum at 266 nm. The band at 211 nm in the UV–vis DRS spectrum (Fig. 5b) of Ti-SBA-15-*pr*-Ade corresponds to the dispersed tetrahedral Ti ions. Adenine could not be deposited directly by impregnation on the unsilynated SBA-15 surface, as it leached out during Soxhlet extraction (see Experimental section) with DMF and CH_3CN. In this case, IR and UV–vis DRS spectral examination of the solid after the extraction did not detect adsorbed adenine. In other words, in the absence of –Cl groups of the 3-chloropropyltriethoxysilane, the adenine cannot be anchored. The $–NH_2$ group of the adenine reacts with the –Cl, eliminating HCl in the process. Hence, adenine is covalently linked through the N–H group to the silynated SBA-15 surface (Scheme 1).

3.4. CO_2 activation

Activation of CO_2 is a key prerequisite for its further participation in chemical reactions. FTIR spectroscopy can identify the structural features of CO_2 in the adsorbed state. In the difference FTIR spectra no *new* peaks are seen when CO_2 is adsorbed on unmodified SBA-15 and Ti-SBA-15

Table 2
FTIR spectral assignments of activated CO_2 species

IR peak position (cm^{-1})	Assignment	Species	IR peak position (cm^{-1})	Assignment	Species
1345	C–O stretching of monodentate carbonate	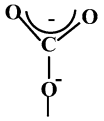	1609 and 1446	Antisymmetric and symmetric C–O stretching vibrations of carbamate anion	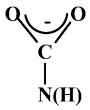
			1622 and 1446	C–O stretching vibrations of carbamate anion (in "neat" adenine)	
1380	C–O stretching vibration of bidentate carbonate	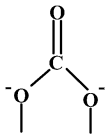	2948 and 2841	C–H stretching vibrations of molecularly adsorbed methanol	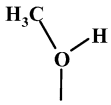
1420	C–O stretching vibration of monodentate bicarbonate	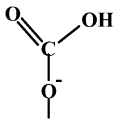	2921 and 2829 1054 and 1030	C–H stretching vibration of methoxides C–H bending modes of methoxide	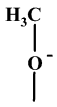
1582	Stretching vibration of methyl carbonate	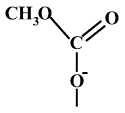	2975 and 2865	C–H stretching vibrations of the bidentate formate species	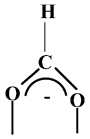
1650	C–O stretching vibration of bidentate bicarbonate	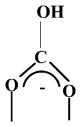			

samples (Fig. 6a). Several new peaks, in the range of 1250–1700 cm^{-1}, are noticed over Ti-SBA-15-*pr*-NH_2, SBA-15-*pr*-Ade, and Ti-SBA-15-*pr*-Ade after exposure to CO_2 (Fig. 6a). For comparison, the difference IR spectrum obtained when CO_2 is adsorbed on "neat" adenine is also given (Fig. 6a). The assignments of these peaks are listed in Table 2. Various activated CO_2 species (carbonates, bicarbonates, carbamates, and formates) are formed on the reaction of activated CO_2 with the species (water, hydroxyls, and amine/adenine) present on the surface. Formation of such activated CO_2 species on metal oxides and zeolites was also noted earlier by several workers [50–53]. CO_2 can also react with the amine (N–H) functionality in SBA-15-*pr*-Ade and Ti-SBA-15-*pr*-Ade to form carbamates [54]. The relative concentration (peak intensity) of the carbamates (IR peaks at 1609 and 1446 cm^{-1}; Fig. 6a and Table 2) is higher than those of other species over these two catalysts (Fig. 6). The following observations are made from the CO_2 adsorption experiments:

1. Unmodified "bare" SBA-15 and Ti-SBA-15 activate CO_2 only weakly.
2. Adenine-modified samples show intense new peaks at 1650, 1609, 1446, 1420, 1380, and 1345 cm^{-1}, corresponding to different activated CO_2 species (Table 2) [50–53]. These peaks are also observed on the propylamine-functionalized SBA-15 and Ti-SBA-15 samples. However, their intensities are much lower than that observed for adenine-modified samples. Thus, the adenine and NH_2 functionalities provide active sites for CO_2 adsorption/activation, with the adenine activating the CO_2 to a greater extent.
3. The intensity of the IR peaks due to the various activated CO_2 species increased with CO_2 pressure (Fig. 6b).
4. IR peaks are more intense at lower temperatures, which is consistent with a higher concentration of adsorbed CO_2 at lower temperatures (Fig. 6c).
5. Solvents have a marked effect. The intensity of the IR peaks is higher in CH_2Cl_2 than in CH_3OH (Fig. 7b). Distinct peaks are noticed in the spectrum of CO_2 adsorbed on Ti-SBA-15-*pr*-Ade in the presence of CH_3OH (Fig. 7a). The peaks at 2948 and 2841 cm^{-1} are associated with molecularly adsorbed CH_3OH [53]. Those at 2921 and 2829 cm^{-1} are due to C–H stretching vibrations of the monodentate and bidentate methoxide groups. The peaks at 2975 and 2865 cm^{-1} (present also in CH_2Cl_2 and ECH preadsorbed samples) are due to C–H stretching vibrations of the bidentate formate species (Fig. 7a). In the case of CH_3OH, new peaks are also observed at 1030 and 1054 cm^{-1} (Fig. 7c), corresponding to the bending modes of the methoxide groups [53].
6. The IR intensities (of CO_2) are also lowered in the presence of an epoxide like epichlorohydrin (ECH), presumably because of their condensation and further conversion to products (Fig. 7b).

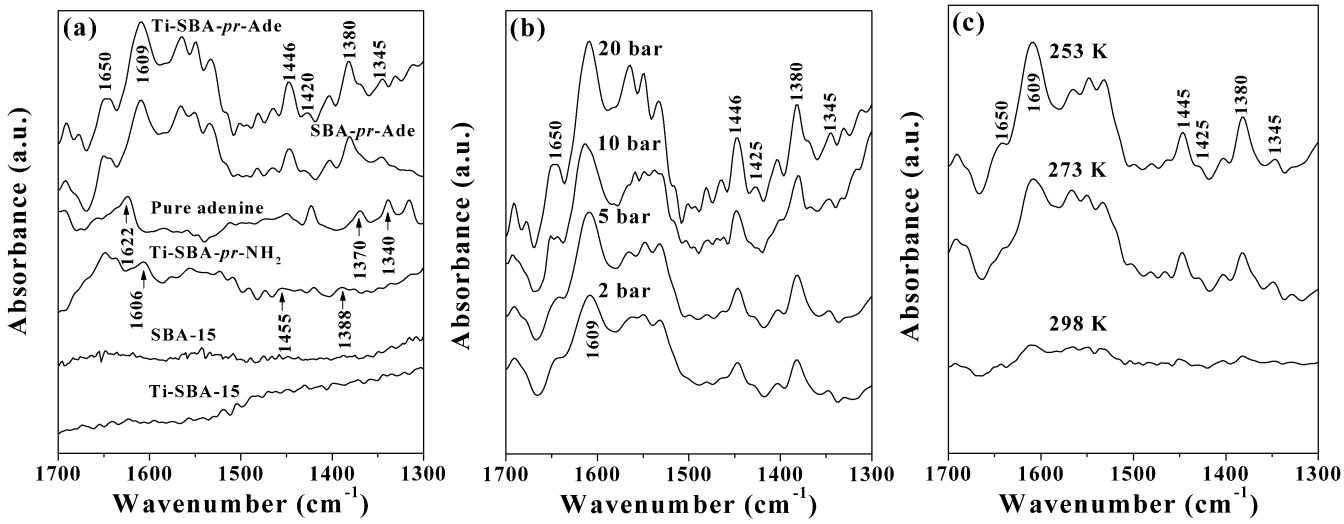

Fig. 6. Difference FTIR spectra recorded after exposure to CO_2. (a) Influence of catalyst – CO_2 pressure, 20 bar; temperature, 253 K. (b) Influence of CO_2 pressure – catalyst, Ti-SBA-15-*pr*-Ade (Si/Ti = 40); temperature, 253 K. (c) Influence of adsorption temperature – catalyst, Ti-SBA-15-*pr*-Ade (Si/Ti = 40); CO_2 pressure, 5 bar. Reaction time is 1 h in all the cases. The spectrum of the sample before CO_2 adsorption was taken as reference. Spectral resolution, 4 cm^{-1}. Number of scans, 100.

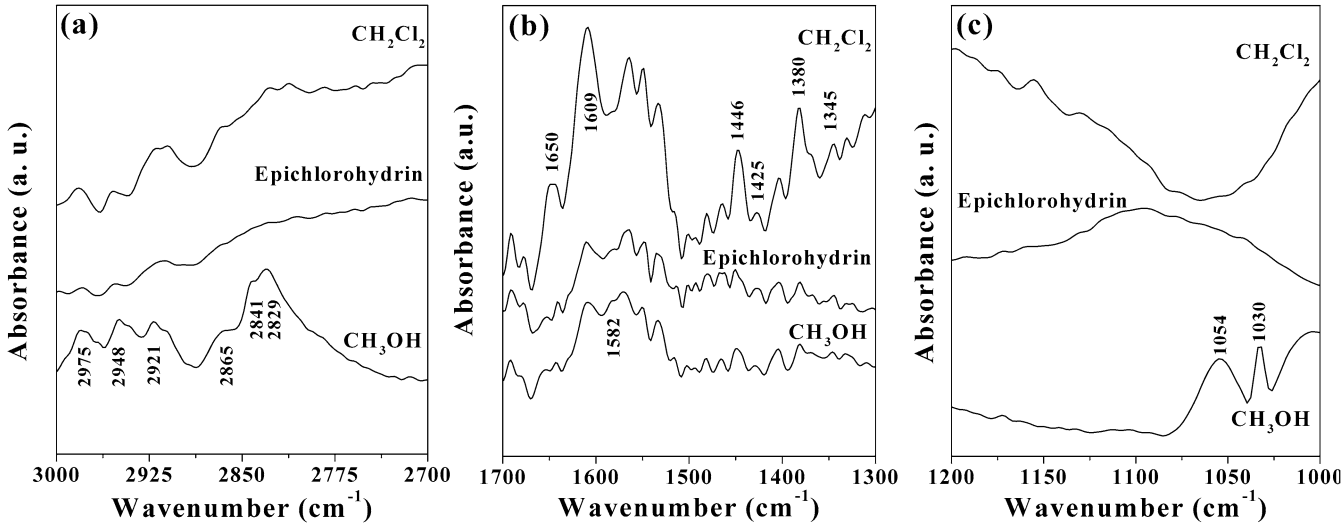

Fig. 7. Difference FTIR spectra of CO_2 adsorbed Ti-SBA-15-*pr*-Ade (Si/Ti = 40) contacted with CH_2Cl_2, epichlorohydrin or CH_3OH. Pressure, 20 bar; temperature, 253 K; reaction time, 1 h. Spectral resolution, 4 cm^{-1}. Number of scans, 100.

The superior catalytic activity of Ti-SBA-15-*pr*-Ade compared with other SBA-15 samples for cyclic carbonate and carbamate synthesis (next section) is in agreement with the above results.

3.5. Catalytic activity

3.5.1. Cyclic carbonate synthesis

Cycloaddition of CO_2 to epoxides yielded the cyclic carbonate as the main product, with the diol and ethers as minor products. Organo-functionalization of SBA-15 with propyl-adenine significantly enhanced the catalytic activity of SBA-15 (Table 3). Bare SBA-15, which was weakly active (ECH conversion = 1.5 mol%), showed ECH conversion of 62.3 mol% after adenine functionalization. The cyclic carbonate selectivity increased from 9 to 83.8 mol% (see entry nos. 1 and 3). A similar increase in the activity (ECH conversion increases from 1.5 to 16.8 mol%) and selectivity (from 9 to 87.5%) was observed also when SBA-15 was titanated (entry nos. 1 and 4). The activity and selectivity were much higher when both Ti and adenine were present (see entry no. 6). The adenine-modified SBA-15 (SBA-15-*pr*-Ade and Ti-SBA-15-*pr*-Ade) showed superior activity compared with the propylamine catalysts (SBA-15-*pr*-NH_2 and Ti-SBA-15-*pr*-NH_2) (compare entry nos. 3 and 6 with 2 and 5, respectively). Moreover, in contrast to all the earlier catalysts, including the commercial processes [30] wherein a significant amount of solvent (dichloromethane) is used

Table 3
Cyclic carbonate synthesis over adenine-modified Ti-SBA-15

Entry No.	Catalyst (Si/Ti)	Epoxide	Run time (h)	Epoxide conversion (%)	Cyclic carbonate selectivity (%)
		Reactions in CH_3CN solvent			
1	SBA-15	Epichlorohydrin	4	1.5	9.0
2	SBA-15-*pr*-NH_2	Epichlorohydrin	4	36.7	89.7
3	SBA-15-*pr*-Ade	Epichlorohydrin	4	62.3	83.8
4	Ti-SBA-15 (40)	Epichlorohydrin	4	16.8	87.5
5	Ti-SBA-15-*pr*-NH_2 (40)	Epichlorohydrin	4	51.5	93.5
6	Ti-SBA-15-*pr*-Ade (40)	Epichlorohydrin	4	84.8	97.7
7	Ti-SBA-15-*pr*-Ade (68)	Epichlorohydrin	4	79.0	90.2
8	Ti-SBA-15-*pr*-Ade (104)	Epichlorohydrin	4	66.0	86.7
9	Ti-SBA-15-*pr*-Ade (40)	Propene oxide	6	95.3	100.0
10	Ti-SBA-15-*pr*-Ade (40)	Styrene oxide	8	79.8	87.0
		Reactions without solvent			
11	SBA-15	Epichlorohydrin	4	15.8	59.0
12	SBA-15-*pr*-Ade	Epichlorohydrin	4	80.5	75.0
13	Ti-SBA-15 (40)	Epichlorohydrin	4	20.1	86.3
14	Ti-SBA-15 (68)	Epichlorohydrin	4	18.7	80.5
15	Ti-SBA-15 (104)	Epichlorohydrin	4	16.0	68.1
16	Ti-SBA-15-*pr*-Cl (40)	Epichlorohydrin	4	19.1	96.4
17	Ti-SBA-15-*pr*-Ade (40)	Epichlorohydrin	4	93.9	89.1
18	Ti-SBA-15-*pr*-Ade (40)	Propene oxide	6	89.2	91.7
19	Ti-SBA-15-*pr*-Ade (40)	Styrene oxide	8	94.0	94.6

Reaction conditions: catalyst, 100 mg in all the SBA-15 catalysts except in entry nos. 2 and 5 where 200 mg was used; epoxide, 18 mmol; solvent, nil or 10 cm^3; CO_2, 6.9 bar; temperature, 393 K. Amine content: SBA-15-*pr*-NH_2 = 2.45 mmol/g catalyst; Ti-SBA-15-*pr*-NH_2 (40) = 2.2 mmol/g catalyst. Adenine content: SBA-15-*pr*-Ade = 1.29 mmol/g catalyst; Ti-SBA-15-*pr*-Ade (40) = 0.91 mmol/g catalyst; Ti-SBA-15-*pr*-Ade (68) = 0.95 mmol/g catalyst; Ti-SBA-15-*pr*-Ade (104) = 0.96 mmol/g catalyst.

in the synthesis of cyclic carbonates, the present catalysts were highly active and selective, even in the absence of any solvent and cocatalysts/promoters (Table 3; see entry nos. 11–19). The higher nucleophilicity and ability to delocalize any ionic charge developed during its interaction with CO_2 may account for the superior catalytic activity of adenine-based catalysts. The higher catalytic activity and selectivity of "neat" adenine in a homogeneous catalytic reaction with ECH as substrate (ECH conversion = 36.6%, chloropropene carbonate selectivity = 89.6%) compared with "neat" propylamine (ECH conversion = 14.9% and chloropropene carbonate selectivity = 84.6%) and "neat" triethoxysilylpropylamine (ECH conversion = 4%, chloropropene carbonate selectivity = 65%) support this hypothesis. These results parallel the higher IR intensities of adsorbed CO_2 on these samples (Fig. 6). ECH conversion increased with an increase in Ti content up to a Si/Ti value of 40 (see entry nos. 6–8 and 13–15). Independent adsorption experiments (10% of ECH in CH_2Cl_2; at 298 K for 1 h) indicated that the adsorption of ECH was increased from 3.4 wt% (SBA-15) to 13.4 wt% for Ti-SBA-15. An important role of Lewis acidic Ti^{4+} ions is to increase the surface concentration of the epoxide molecules, thereby enhancing the catalytic activity. Cyclic carbonate selectivity was also much lower on "bare" SBA-15.

Ti-SBA-15-*pr*-Ade was active for cycloaddition of CO_2 with a variety of epoxides of different sizes and structures (Table 3). Styrene oxide, for example, could be converted into styrene carbonate in high yields over these catalysts (epoxide conversion = 94% and cyclic carbonate selectivity = 94.6%; entry no. 19).

Both epoxide conversion and carbonate yields increased at higher pressures (Fig. 8). The increase in conversion and yield correlated with the intensity of the peak at 1609 cm^{-1} (Fig. 8) due to CO_2 activated at the amine sites, highlighting the importance of such sites for CO_2 activation.

Even though the cycloadditions could be carried out in the absence of solvents over these catalysts with high conversions and selectivities as illustrated in Table 3, the use of solvents was found to prolong catalyst life significantly (compare Figs. 9a and b). When cycloaddition was carried out in the *presence* of solvents, the catalysts could be reused (after filtration and drying at 353 K) in several recycling experiments with little loss in activity or selectivity (Fig. 9a). However, when the same reactions were conducted in the *absence* of any solvent, a progressive decrease in catalytic activity (but not selectivity) was observed in successive runs, as shown in Fig. 9b. To explore the cause of this deactivation, the catalyst, after the seventh recycle experiment (Fig. 9b, conversion = 48.2%), was washed first with acetonitrile and then with acetone and dried at 383 K for 1 h. The color of the catalyst, which was dark brown before this solvent extraction, was almost restored to its original off-white color. The dark brown extract contained some heavy products. In the subsequent cycloaddition (eighth recycle, Fig. 9b), the conversion increased to 84.0%. One of the main roles of the solvents is, hence, to continuously remove the carbonaceous deposits from the catalyst surface and keep it clean. After

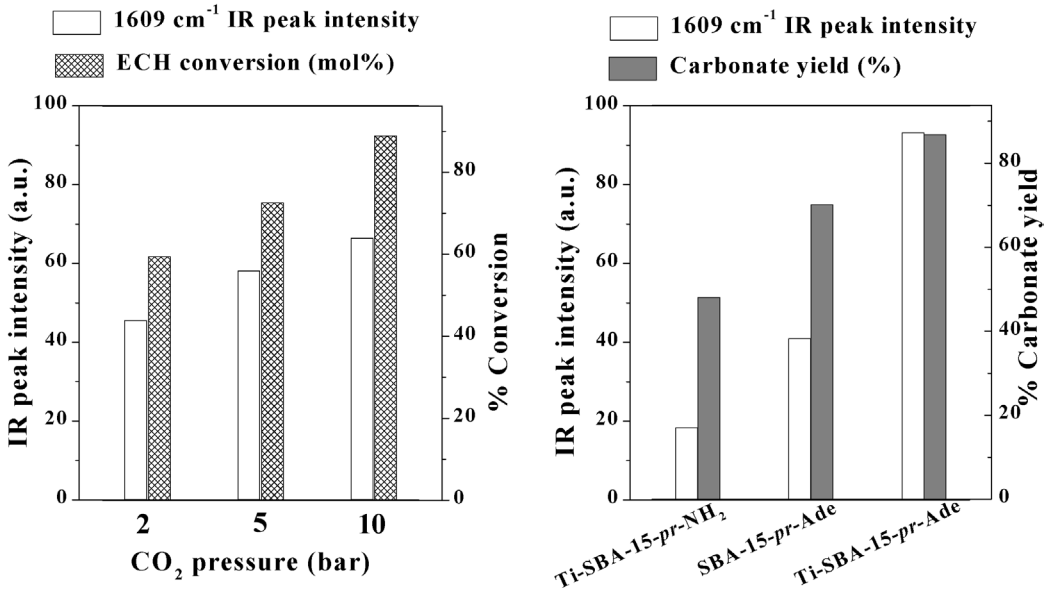

Fig. 8. Left: Correlation between IR peak (1609 cm^{-1}) intensity and epichlorohydrin (ECH) conversion over Ti-SBA-15-*pr*-Ade (Si/Ti = 40) at different CO_2 pressures. Right: Correlation between IR peak (1609 cm^{-1}) intensity and chloropropene carbonate yield over different solid catalysts.

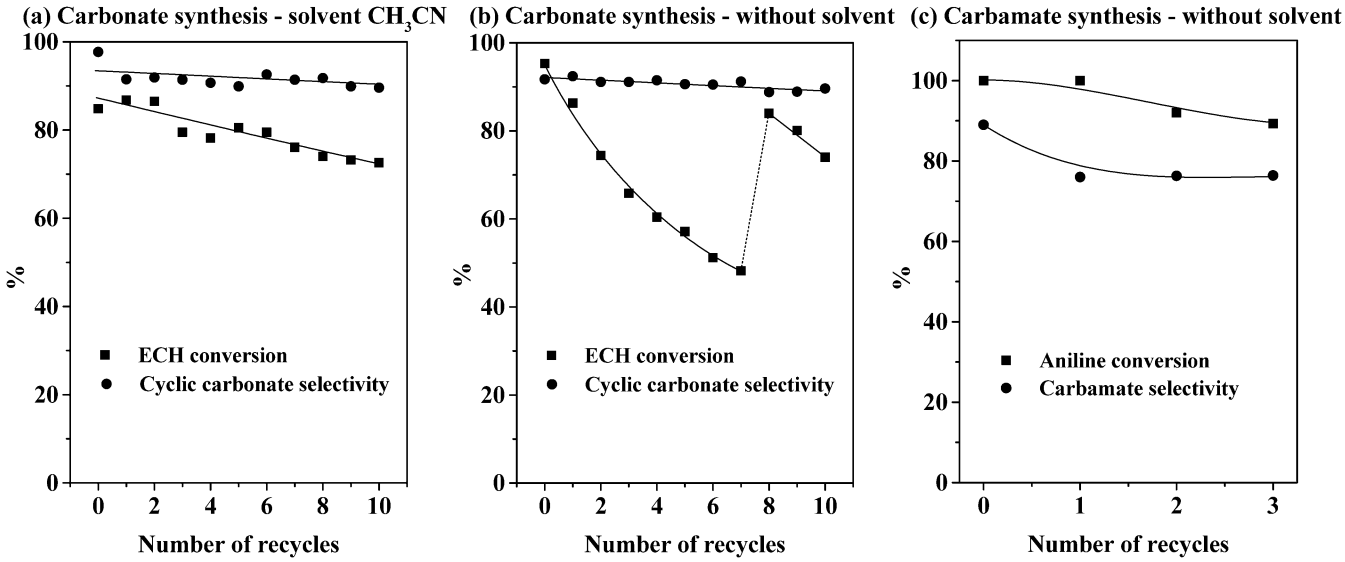

Fig. 9. Catalytic activity of Ti-SBA-15-*pr*-Ade (Si/Ti = 40) in recycling experiments. (a) Cyclic carbonate synthesis in the presence of solvent CH_3CN, (b) cyclic carbonate synthesis in the absence of solvent, (c) *n*-Butyl-N-phenyl carbamate synthesis in the absence of solvent.

the tenth recycle experiment, the catalyst was analyzed for Ti and amine contents (by AAS and elemental analysis, respectively). There was no change in the Ti content. Ti could not be detected in either the reaction mixtures or the solvent extracts. These results indicate that the major cause of catalyst deactivation was not the leaching of Ti. Active site pore blocking by the residual carbonaceous matter is probably the reason.

The Mg/Al oxide-based catalyst system reported earlier [17], for example, required a high catalyst loading of 1.8 g/g of substrate and, in addition, a substantial amount of solvent (85% v/v DMF) and longer reaction times (24 h). Silica-supported guanidine catalysts [26] also required longer reaction times (70 h) and high pressures (50 bar). In contrast, the adenine-functionalized Ti-SBA-15 system reported in the present study requires only 0.06 g of catalyst/g of substrate. Under our experimental conditions (ECH, 20 mmol; CO_2, 6.9 bar; temperature, 393 K; reaction time, 4 h) MgO (800 mg, Aldrich Co.) showed an ECH conversion of 17.3% and a cyclic carbonate selectivity of 2.9%. Under these conditions Mg/Al oxide (Mg/Al = 5) prepared per the reported procedure [17] showed an ECH conversion of 10% and a cyclic carbonate selectivity of 17.5%. In other words, the activities of both MgO and Mg/Al oxide reported by others [17] are considerably lower than that obtained over our adenine modified-Ti-SBA-15 catalysts (Table 3; entry no. 17).

Table 4
Carbamate synthesis over adenine-modified SBA-15 in the absence of solvent

Entry No.	Catalyst (Si/Ti)	Amines	Run time (h)	Amine conversion (%)	Product selectivity (%)	
					Carbamate	N,N-Dialkylation
1	SBA-15	Aniline	4	16.5	81.1	18.9
2	SBA-15-*pr*-NH_2	Aniline	4	20.0	94.8	5.2
3	SBA-15-*pr*-Ade	Aniline	4	44.2	87.3	12.7
4	SBA-15-*pr*-Ade	Aniline	10	99.4	77.9	22.1
5	Ti-SBA-15 (40)	Aniline	4	48.1	79.1	20.9
6	Ti-SBA-15 (68)	Aniline	4	32.9	78.2	21.8
7	Ti-SBA-15 (104)	Aniline	4	26.5	79.3	20.7
8	Ti-SBA-15-*pr*-Cl (40)	Aniline	4	51.2	83.2	16.8
9	Ti-SBA-15-*pr*-NH_2 (40)	Aniline	4	61.6	69.1	30.9
10	Ti-SBA-15-*pr*-Ade (40)	Aniline	4	100	89.0	11.0
11	Ti-SBA-15 (40)	2,4,6-Trimethylaniline	4	21.8	87.4	12.6
12	SBA-15-*pr*-Ade	2,4,6-Trimethylaniline	4	32.5	93.5	6.5
13	Ti-SBA-15-*pr*-Ade (40)	2,4,6-Trimethylaniline	4	74.5	87.8	12.4
14	SBA-15-*pr*-Ade	Benzylamine	4	62.0	98.0	2.0
15	Ti-SBA-15-*pr*-Ade (40)	Benzylamine	4	88.6	92.8	7.2
16	SBA-15-*pr*-Ade	Cyclohexylamine	4	91.0	83.5	16.5
17	SBA-15-*pr*-Ade	Hexylamine	4	96.5	88.0	12.0
18	SBA-15-*pr*-Ade	Octylamine	4	98.8	93.5	6.5

Reaction conditions: catalyst, 100 mg; amine, 10 mmol; *n*-butyl bromide, 12 mmol; CO_2, 3.4 bar; solvent, nil; temperature, 353 K. Amine content: SBA-15-*pr*-NH_2 = 2.45 mmol/g catalyst; Ti-SBA-15-*pr*-NH_2 (40) = 2.2 mmol/g catalyst. Adenine content: SBA-15-*pr*-Ade = 1.29 mmol/g catalyst; Ti-SBA-15-*pr*-Ade (40) = 0.91 mmol/g catalyst; Ti-SBA-15-*pr*-Ade (68) = 0.95 mmol/g catalyst; Ti-SBA-15-*pr*-Ade (104) = 0.96 mmol/g catalyst.

3.5.2. Alkyl and aryl carbamates

Various alkyl and aryl carbamates could be synthesized under mild conditions by reaction of amines, CO_2, and *n*-butyl bromide over modified Ti-SBA-15 catalysts (Table 4). The reaction yielded butyl-N-phenyl carbamate as the major product and N,N′-dibutylamine (N-alkylation) as the minor product. The reaction of CO_2 with a primary amine yields the carbamate anion. This, in turn, reacts with alkyl halides, yielding the corresponding carbamate [Eq. (2)]. However, in the absence of an efficient catalyst, the reaction of a carbamate anion with alkyl halide yields predominantly the nitrogen-derived products [45].

Both aliphatic and aromatic amines could be converted into their corresponding carbamates. Aliphatic amines could be more easily converted. The carbamate yields decreased in the order octylamine > hexylamine > cyclohexylamine > benzylamine > aniline > 2,4,6 trimethylaniline (Table 4). With most of the hitherto known catalyst systems, the reaction occurs in the presence of a solvent like DMF. In the absence of solvents, the N-alkylated compound was the main product. Interestingly, over Ti-SBA-15-*pr*-Ade catalysts, carbamate product could be obtained in high selectivity (84–95%), even without any solvent (Table 4).

SBA-15 alone is only weakly active (Table 4, entry no. 1). The catalytic activity is enhanced upon titanation (see entry nos. 5–7). A slight enhancement in activity was observed upon adenine functionalization (see entry no. 3). When both Ti and adenine were present, the catalytic activity was much higher, and complete conversion of amine (aniline) was observed (see entry no. 10). Similar conversions could be achieved even on SBA-15-*pr*-Ade catalysts but at longer hours (10 h instead of 4 h) (compare entry nos. 3 and 4). When both Ti and adenine were present (Ti-SBA-15-*pr*-Ade), there was a synergistic effect that significantly enhanced the conversion (see entry nos. 3, 5, and 10–13). Even in this reaction we found that the substrate (aniline) conversion increased with a decrease in the Si/Ti ratio up to a value of 40. The adenine-modified Ti-SBA-15 showed superior activity compared with the propyl amine and propyl chloride catalysts (compare entry nos. 8–10). Fig. 9c shows the efficiency of the Ti-SBA-15-*pr*-Ade catalyst system for carbamate synthesis from aniline, CO_2, and *n*-butyl bromide in three recycling experiments. Deposition of carbonaceous matter is also likely to be the cause of catalyst deactivation in this case.

As indicated in Tables 3 and 4, both the titanium ions (weak Lewis acid sites) and the amine moieties (the basic sites) are necessary for maximum catalyst activity and selectivity. We attempted to quantify the relationship between the concentration of these sites and conversion by calculating the turnover frequency (TOF) values. Even though the calculation of TOF values is not unambiguous in our case, where the “active sites” comprise two structurally different surface species (acidic Ti ions and basic amine moieties) and the rate-determining step is not known with certainty, such values can be of use in determining the relative importance of the two sites and, thereby, lead to the design of superior catalysts. Table 5 presents TOF values per acid site (moles of substrate converted per mole of NH_3 desorbed per hour) or per basic site (moles of substrate converted per mole of CO_2 desorbed per hour). Samples that contain the more basic adenine molecule and those that contain both Ti and an adenine molecule have higher intrinsic catalytic activity. It should be borne in mind that the TOFs in Table 5 are the

Table 5
Turnover frequencies (TOF) for chloropropene carbonate and *n*-butyl-N-phenyl carbamate synthesis over Ti-SBA-15 catalyst systems

Catalyst	CO_2 desorbed (mmol/g catalyst)	NH_3 desorbed (mmol/g catalyst)	TOF (h^{-1})[a]			
			Chloropropene carbonate synthesis		*n*-Butyl-N-phenyl carbamate	
			Based on CO_2 desorbed[b]	Based on NH_3 desorbed[c]	Based on CO_2 desorbed[d]	Based on NH_3 desorbed[e]
Ti-SBA-15 (Si/Ti = 40)	2.9	0.9	–	8.5	–	13.8
SBA-15-*pr*-NH_2	3.8	–	2.3	–	1.4	–
Ti-SBA-15-*pr*-NH_2 (Si/Ti = 40)	3.9	0.9	3.0	24.5	3.9	15.9
SBA-15-*pr*-Ade	4.3	–	6.5	–	2.5	–
Ti-SBA-15-*pr*-Ade (Si/Ti = 40)	5.3	1.0	7.3	35.6	4.7	23.2

[a] TOF values are calculated from the conversions reported in Tables 3 and 4.
[b] TOF = moles of epichlorohydrin converted per mole of CO_2 desorbed per h.
[c] TOF = moles of epichlorohydrin converted per mole of NH_3 desorbed per h.
[d] TOF = moles of aniline converted per mole of CO_2 desorbed per h.
[e] TOF = moles of aniline converted per mole of NH_3 desorbed per h.

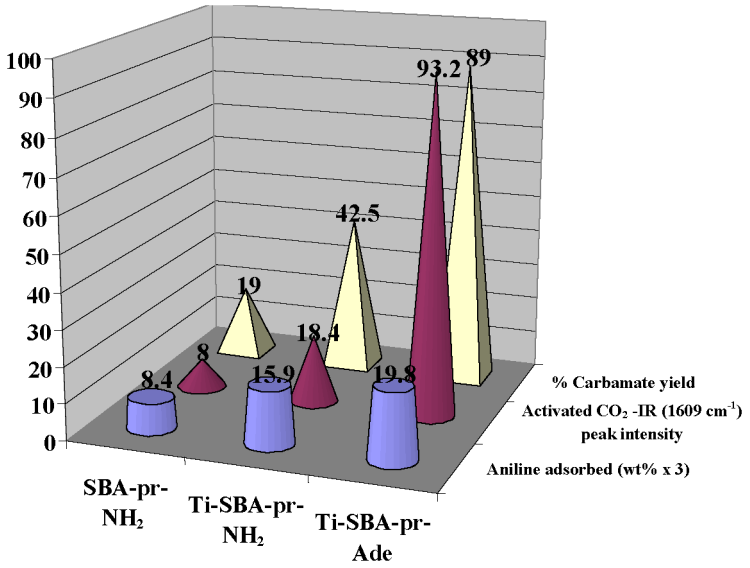

Fig. 10. Correlation of *n*-butyl-N-phenyl carbamate yield with the amount of aniline adsorbed (×3, wt%) and carbamate IR peak intensity (1609 cm^{-1}) over different solid catalysts.

minimum values, since many of the sites, from which CO_2 or NH_3 desorb, may not participate in the catalytic reaction.

We have also carried out the aniline adsorption studies on different catalyst supports. The study reveals that aniline adsorption is higher when Ti (Lewis acid) is present in the catalyst. The carbamate yield increases with an increase in the amount of available adsorbed aniline. It may be recalled that DRIFTIR spectroscopy of adsorbed CO_2 on various catalysts (Fig. 6) had indicated that CO_2 activation (based on the intensity of the carbamate peak at 1609 cm^{-1}) takes place only in the case of propylamine- and adenine-functionalized SBA-15 and Ti-SBA-15 supports. Pure SBA-15 or Ti-SBA-15 could not activate CO_2. Furthermore, the amounts of activated CO_2 were higher in the case of adenine-functionalized supports than in the case of propylamine-functionalized supports. In other words, whereas the Ti ions adsorb the epoxides or the alkyl or aryl amines, the adenine functionality activates CO_2. Accordingly, the carbamate yields correlate with the availability of the adsorbed aniline and activated CO_2 (Fig. 10).

The main features of our catalytic data are the following:

1. Catalytic activity of Ti-SBA-15 is more than that of SBA-15. Ti^{4+} ions enhance the adsorption and surface concentration of the substrate, with ECH leading to the observed increase in activity. In the absence of basic sites to activate the other reactant, CO_2, however, the catalytic activity is low.
2. For the insertion of CO_2 into organic molecules, like epoxides and anilines, it first has to be activated. CO_2, a weak Lewis acid, is activated on the basic sites of adenine (or other amines). Hence, silicate samples containing adenine, like SBA-15-*pr*-Ade, are more active than those (like SBA-15), which do not contain the base.

However, in the absence of Ti^{4+} ions, which adsorb and retain the epoxide molecules, the increase in activity is only modest. Catalytic activity is enhanced at higher partial pressures of CO_2 (Fig. 8), which increases the surface concentration of CO_2.

3. When the Ti^{4+} ions and the basic adenine functionalities coexist on the same surface, activated CO_2 molecules and Lewis acid-bound epoxides (or the anilines) are generated simultaneously, and the condensation reaction occurs, leading to the products (cyclic carbonates or carbamates). This is the reason for the increase in catalytic activity with Ti content and with the surface concentration of the activated CO_2 species (as inferred from IR spectroscopy).
4. Even though both acidic and basic sites are needed for the insertion of CO_2 in epoxides and amines, the activation of CO_2 at basic sites (the grafted amine moieties in our case) is of greater importance in determining catalyst activity.

4. Conclusions

A highly active and reusable solid catalyst (adenine-modified Ti-SBA-15) for the synthesis of cyclic carbonates (from epoxides and CO_2) and alkyl and aryl carbamates (from amines, *n*-butyl bromide, and CO_2) is reported. High yields of the products are obtained even in the absence of solvents. In the case of cyclic carbonate synthesis the reaction proceeds without any additional cocatalysts like DMAP and quaternary ammonium salts. The process using the present catalyst system avoids hazardous substances like phosgene or isocyanate and occurs at low temperatures and pressures.

Acknowledgments

R.S. acknowledges the Council of Scientific and Industrial Research (CSIR), New Delhi, for a fellowship. This work forms a part of the Network project Catalysts and Catalysis (P23-CMM005.3), sponsored by CSIR, New Delhi.

References

[1] H. Arakawa, M. Aresta, J.N. Armor, M.A. Barteau, E.J. Beckman, A.T. Bell, J.E. Bercaw, C. Creutz, E. Dinjus, D.A. Dixon, K. Domen, D.L. DuBois, J. Eckert, E. Fujita, D.H. Gibson, W.A. Goddard, D.W. Goodman, J. Keller, G.J. Kubas, H.H. Kung, J.E. Lyons, L.E. Manzer, T.J. Marks, K. Morokuma, K.M. Nicholas, R. Periana, L. Que, J. Rostrup-Nielson, W.M.H. Sachtler, L.D. Schmidt, A. Sen, G.A. Somorjai, P.C. Stair, B.R. Stults, W. Tumas, Chem. Rev. 101 (2001) 953.
[2] T. Inui, M. Anpo, K. Izui, S. Yanagida, T. Yamaguchi (Eds.), Advances in Chemical Conversions for Mitigating Carbon Dioxide, Studies in Surface Science and Catalysis, vol. 114, Elsevier, New York, 1998.
[3] A. Behr, Angew. Chem. Int. Ed. Engl. 27 (1988) 661.
[4] B. Elvers, S. Hawkins, G. Schulz (Eds.), Ulmann's Encyclopedia of Industrial Chemistry A, vol. 21, fifth ed., VCH, Weinheim, Germany, 1992, p. 207.
[5] S. Inoue, H. Koinuma, T. Tsuruta, Polymer Lett. 7 (1969) 287.
[6] S. Inoue, CHEMTECH (1976) 588.
[7] E.J. Beckman, Science 283 (1999) 946.
[8] R. Nomura, A. Ninagawa, H. Matsuda, J. Org. Chem. 45 (1980) 3735.
[9] A.-A.G. Shaikh, S. Sivaram, Chem. Rev. 96 (1996) 951.
[10] D.J. Darensbourg, M.W. Holtcamp, Coor. Chem. Rev. 153 (1996) 155.
[11] D.J. Daresbourg, J.C. Yarbrough, J. Am. Chem. Soc. 124 (2002) 6335.
[12] M. Cheng, D.R. Moore, J.J. Reczek, B.M. Chamberlain, E.B. Lobkovsky, G.W. Coates, J. Am. Chem. Soc. 123 (2001) 8738.
[13] H. Kawanami, Y. Ikushima, Chem. Commun. (2000) 2089.
[14] T. Nishikubo, A. Kameyama, J. Yamashita, M. Tomoi, W. Fukuda, J. Polym. Sci. Part A: Polym. Chem. 31 (1993) 939.
[15] T. Yano, H. Matsui, T. Koike, H. Ishiguro, H. Fujihara, M. Yoshihara, T. Maeshima, Chem. Commun. (1997) 1129.
[16] B.M. Bhanage, S.-i. Fujita, Y. Ikushima, M. Arai, Appl. Catal. A: Gen. 219 (2001) 259.
[17] K. Yamaguchi, K. Ebitani, T. Yoshida, H. Yoshida, K. Kaneda, J. Am. Chem. Soc. 121 (1999) 4526.
[18] M. Aresta, A. Dibenedetto, L. Gianfrate, C. Pastore, Appl. Catal. A: Gen. 255 (2003) 5.
[19] H. Yasuda, L.-N. He, T. Sakakura, J. Catal. 209 (2002) 547.
[20] M. Tu, R.J. Davis, J. Catal. 199 (2001) 85.
[21] E.J. Doskocil, S.V. Bordawekar, B.G. Kaye, R.J. Davis, J. Phys. Chem. B 103 (1999) 6277.
[22] H.S. Kim, J.J. Kim, H.N. Kwon, M.J. Chung, B.G. Lee, H.G. Jang, J. Catal. 205 (2002) 226.
[23] J. Peng, Y. Deng, New J. Chem. 25 (2001) 639.
[24] H. Kawanami, A. Sasaki, K. Matsui, Y. Ikushima, Chem. Commun. (2003) 896.
[25] H.S. Kim, J.J. Kim, H. Kim, H.G. Jang, J. Catal. 220 (2003) 44.
[26] A. Barbarini, R. Maggi, A. Mazzacani, G. Mori, G. Sartori, R. Sartorio, Tetrahedron Lett. 44 (2003) 2931.
[27] X.-B. Lu, Y.-J. Zhang, K. Jin, L.-M. Luo, H. Wang, J. Catal. 227 (2004) 537.
[28] X.-B. Lu, H. Wang, R. He, J. Mol. Catal. 186 (2002) 33.
[29] Filtration Industry Analyst 1999 (Issue No. 27, June 1999) 2.
[30] S. Fukuoka, M. Kawamura, K. Komiya, M. Tojo, H. Hachiya, K. Hasegawa, M. Aminaka, H. Okamoto, I. Fukawa, S. Konno, Green Chem. 5 (2003) 497.
[31] R. Srivastava, D. Srinivas, P. Ratnasamy, Catal. Lett. 91 (2003) 133.
[32] R. Srivastava, D. Srinivas, P. Ratnasamy, Catal. Lett. 89 (2003) 81.
[33] R. Srivastava, D. Srinivas, P. Ratnasamy, in: E.W.J. van Steen, L.H. Callanan, M. Claeys, C.T. O'Connor (Eds.), Recent Advances in the Science and Technology of Zeolites and Related Materials, Proceeding of the 14th International Zeolite Conference, Cape Town, South Africa (April 24–30, 2004), Elsevier, Amsterdam, The Netherlands, 2004, pp. 2703–2710.
[34] P. Adams, F.A. Baron, Chem. Rev. 65 (1965) 567.
[35] J.J. McKetta, W.A. Cunningham (Eds.), Encyclopedia of Chemical Processing and Design, vol. 20, Decker, New York, 1984, p. 117.
[36] B. Elvers, S. Hawkins, G. Schulz (Eds.), Ullman's Encyclopedia of Industrial Chemistry A, vol. 21, fifth ed., VCH, Weinheim, German, 1992, p. 207.
[37] T. Takeuchi, M. Nishi, T. Irie, H. Ryuto, US Patent 4,469,882 (1984).
[38] R.V. Chaudhari, S.P. Gupte, A.A. Kelkar, D.S. Kolhe, US Patent 5,502,241 (1996).
[39] S.P. Gupte, R.V. Chaudhari, J. Catal. 114 (1998) 246.
[40] Y. Matsumura, T. Maki, Y. Satoh, Tetrahedron Lett. 38 (1997) 8879.
[41] F. Shi, J. Peng, Y. Deng, J. Catal. 219 (2003) 372.
[42] W. McGhee, D. Riley, K. Christ, Y. Pan, B. Parnas, J. Org. Chem. 60 (1995) 2820.
[43] I. Vauthey, F. Valot, C. Gozzi, F. Fache, M. Lamaire, Tetrahedron Lett. 41 (2000) 6347.
[44] D.B. Dell'Amico, F. Calderazzo, L. Labella, F. Marchetti, G. Pampaloni, Chem. Rev. 103 (2003) 3857.

[45] R. Srivastava, M.D. Manju, D. Srinivas, P. Ratnasamy, Catal. Lett. 97 (2004) 41.
[46] D. Zhao, J. Feng, Q. Huo, N. Melosh, G.H. Fredrickson, B.F. Chmelka, G.D. Stucky, Science 279 (1998) 548.
[47] P. Wu, T. Tatsumi, T. Komatsu, T. Yashima, Chem. Mater. 14 (2002) 1657.
[48] P. Sutra, D. Brunel, Chem. Commun. (1996) 2485.
[49] X.-G. Zhou, X.-Q. Yu, J.-S. Huang, S.-G. Li, L.-S. Li, C.-M. Che, Chem. Commun. (1999) 1789.
[50] F. Solymosi, H. Knözinger, J. Catal. 122 (1990) 166.
[51] K. Tomishige, Y. Ikeda, T. Sakaihori, K. Fujimoto, J. Catal. 192 (2000) 355.
[52] R. Bal, B.B. Tope, T.K. Das, S.G. Hegde, S. Sivasanker, J. Catal. 204 (2001) 358.
[53] K.T. Jung, A.T. Bell, J. Catal. 204 (2001) 339.
[54] A.C.C. Chang, S.S.C. Chuang, M. Gray, Y. Soong, Engery & Fuels 17 (2003) 468.